MICROWAVE APPLICATIONS OF TRANSMISSION-LINE BASED NEGATIVE REFRACTIVE INDEX STRUCTURES

C. CALOZ, A. SANADA, AND T. ITOH
Electrical Engineering Department, University of California, Los Angeles
405 Hilgard Ave., Los Angeles, CA90095-1594, USA
E-mail: caloz@ee.ucla.edu, sanada@ee.ucla.edu, itoh@ee.ucla.edu

This paper presents the fundamental theory and practical implementation of metamaterials and, more specifically, of composite right/left-handed (CRLH) structures. Four different applications developed at UCLA are presented: a dual-band branch-line coupler, a coupled-line tight backward coupler, a backfire-to-endfire leaky-wave antenna and a planar distributed negative-refractive-index lens.

1. Introduction

Recently, there has been considerable interest for novel metamaterials, and in particular for left-handed (LH) materials, which are characterized by anti-parallel phase and group velocities [1]-[2].

Our group at UCLA has introduced the concept of composite right/left-handed (CRLH) structures, after recognizing that a purely LH structure cannot exist in nature because it necessarily includes parasitic right-handed (RH) effects [3]-[4]. This concept, based on a transmission line approach [5], has lead to the development of an original theory and of several novel microwave applications.

This paper presents the fundamental theory and practical realization of CRLH structures, and demonstrates four specific applications of these structures.

2. CRLH Structures Theory

All practical LH structures include RH parasitic effects, and are therefore composite right/left-handed in reality (CRLH).

2.1. Transmission Line Model

An ideal CRLH-TL is represented in Fig. 1 by its circuit model.

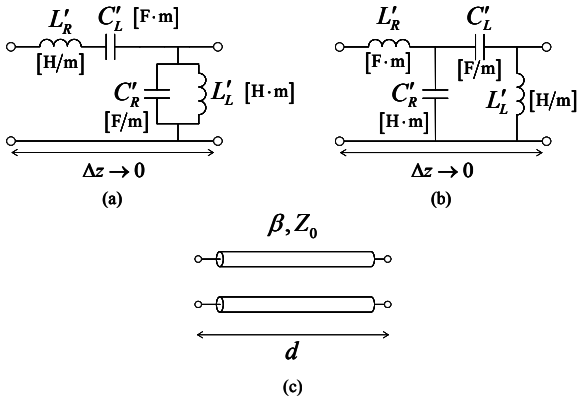

Figure 1: Ideal CRLH-TL. (a) Infinitesimal circuit model. (b) Equivalent infinitesimal circuit model in the balanced case ($L_R'C_L' = L_L'C_R'$). (c) Line representation and physical parameters. The subscripts R and L stand for RH and LH, respectively.

The most appropriate model in practice is the one of Fig. 1a, which has the dispersion relation

$$\beta = s(\omega)\sqrt{\omega^2 L'_R C'_R + \frac{1}{\omega^2 L'_L C'_L} - \left(\frac{L'_R}{L'_L} + \frac{C'_R}{C'_L}\right)}, \quad (1a)$$

where

$$s(\omega) = \begin{cases} -1 \text{ if } \omega < \omega_{\Gamma 1} = \min\left(\dfrac{1}{\sqrt{L'_R C'_L}}, \dfrac{1}{\sqrt{L'_L C'_R}}\right) \\ +1 \text{ if } \omega > \omega_{\Gamma 2} = \max\left(\dfrac{1}{\sqrt{L'_R C'_L}}, \dfrac{1}{\sqrt{L'_L C'_R}}\right) \end{cases} \quad (1b)$$

from which all the parameters Z_0, v_p, v_g, t_g can be straightforwardly derived in a closed form. (The reason for the frequency-dependent sign function $s(\omega)$ will become clear in Sec. 2.2 and

Fig. 4.) However, it can be easily verified that in the particular *balanced* case, defined as

$$L'_R C'_L = L'_L C'_R = L'C' , \qquad (2)$$

the model of Fig. 1a is equivalent to the model of Fig. 1b, which is simpler and provides a more direct insight into the physical properties of CRLH structures. The corresponding dispersion relation,

$$\beta_s = \beta_R + \beta_L = \omega^2 L'_R C'_R - \frac{1}{\omega^2 L'_L C'_L} , \qquad (3)$$

emphasizes the dual nature of metamaterials, which exhibit LH characteristics at low frequency and RH characterisitics at high frequencies, with a transition frequency given in general by

$$\omega_0 = \frac{1}{\sqrt[4]{L'_R C'_R L'_L C'_L}} \overset{\text{balanced}}{=} \frac{1}{\sqrt{L'C'}} , \qquad (4)$$

where $\beta = 0$, and therefore $\lambda_g = \infty$. If the structure is unbalanced *($L_R'C_L' \neq L_L'C_R'$)*, and therefore mismatched, a gap opens up in some frequency range, due to the negative sign appearing in the radicand of (1); in this case, (4) can be shown to represent the frequency of largest attenuation in the gap. Moreover, it can be easily verified from the model of Fig. 1b and equation (1), that

$$v_g(\omega \to \infty) = \frac{1}{\sqrt{L'_R C'_R}} = \frac{c_0}{n} , \qquad (5)$$

which clearly show that group velocity is bounded by c_0/n in a CRLH structure. It is also interesting to note that in the *balanced* case

$$v_g(\omega = \omega_0) = \frac{1}{2\sqrt{L'C'}} = \frac{c_0}{2n} . \qquad (6)$$

These results contrast with the purely LH-TL (including only series C and shunt L), which cannot exist physically because its group velocity is unbounded. In the *unbalanced* case, a gap opens up between the LH and RH bands, but the asymptotic value $\omega \to \infty$ of v_g is still c_0/n because the LH components become insignificant in the model of Fig. 1a. These results for phase and group velocities are illustrated in Fig. 2.

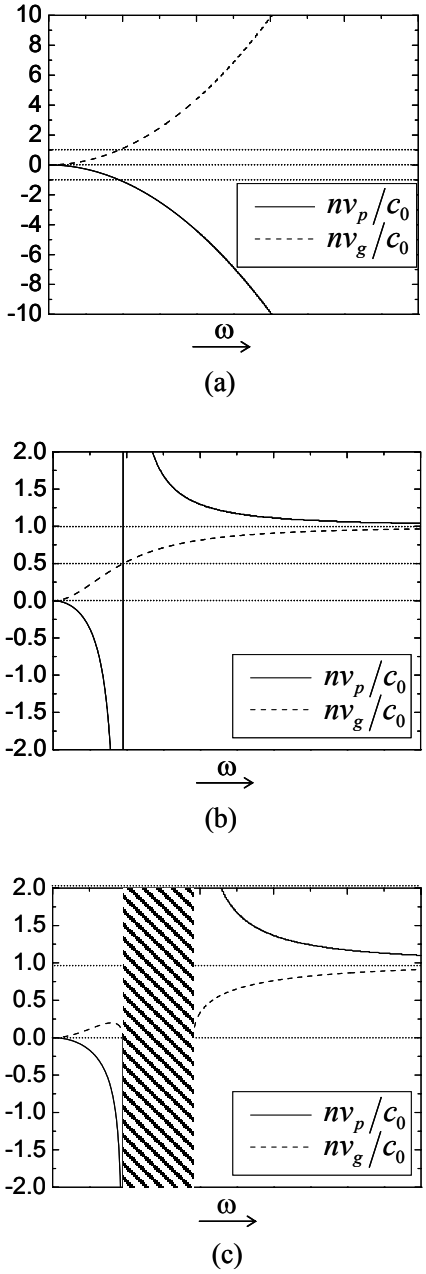

Figure 2: Phase and group velocities. (a) Purely LH-TL (non-physical). (b) Balanced CRLH-TL, from (1) or (3). (c) Unbalanced CRLH-TL, from (1).

2.2. Periodic-Network Realization

A CRLH-TL can be synthesized in the form of a periodic ladder-network with the band-pass unit cell shown in Fig. 3 in condition that this unit cell is electrically small enough to approximate the incremental model of Fig. 1a. It should be noted that, since the unit cell is much smaller than 180° (Bragg regime), the CRLH-TL is essentially "seen" as a *homogeneous* TL, or an *effective* medium, by EM waves. Therefore, periodicity is in fact not a necessity, but a

computational and fabrication convenience. The electric characteristics (cutoff and transition frequencies, impedance, phase shift, group delay, etc.) of the unit cell of Fig. 3 can be straightforwardly derived by conventional circuit theory.

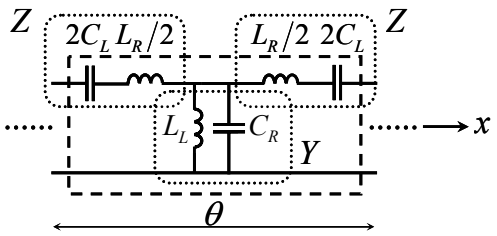

Figure 3: Unit cell of a periodic-network realization of a 1D CRLH-TL. The inductances L_R / L_L and capacitances C_R / C_L are in H and F, respectively. θ represents the electrical length of the cell.

If the structure is periodic, the Bloch-Floquet theorem can be used to relate the input/output currents/voltages of the unit cell. By using in addition, a transmission matrix formalism and Kirchoff's laws for the unit cell, we obtain the following analytical dispersion relation for the CRLH-TL

$$\cos(\beta a) = 1 - \frac{1}{2}\left[\frac{1}{\omega^2 L_L C_L} + \omega^2 L_R C_R - \left(\frac{L_R}{L_L} + \frac{C_R}{C_L}\right)\right] \quad (7)$$

which is plotted in Fig. 4. This dispersion diagram is the keystone of CRLH structures. Continuous transition between the LH and RH branches with non-zero group velocity can be achieved in the balanced case. These branches partly extend beyond the air line, where they are leaky when the structure is open (exploited in the leaky-wave antenna of Sec. 3.3), while they are purely guided below the air line.

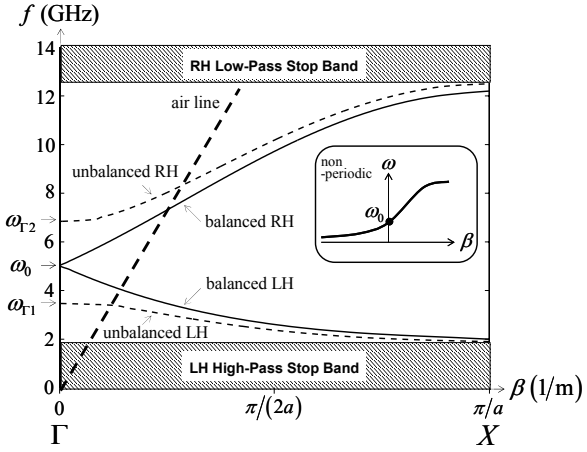

Figure 4: Dispersion relation computed for the balanced and unbalanced CRLH-TL. Balanced: L_R = L_L = 1 nH, C_R = C_L = 1 pF; unbalanced: L_R = 1 nH, L_L = 5.5 nH, C_R = 1 pF, C_L = 2 pF. The inset shows the dispersion curve of a balanced non periodic CRLH-TL.

The 1D-CRLH-TL can be straightforwardly extended to a 2D-CRLH (or even 3D) network, with the unit cell shown in Fig. 5. The same type of analysis as for 1D, but using this time periodic boundary conditions along both x and y directions, leads to the analytical dispersion relation

$$\frac{\left(e^{-jk_x a} - 1\right)^2}{e^{-jk_x a}} + \frac{\left(e^{-jk_y a} - 1\right)^2}{e^{-jk_y a}} - 2ZY = 0, \quad (8)$$

where

$$Z = \frac{1}{2}\left(\frac{1}{j\omega C_L} + j\omega L_R\right), \quad Y = \frac{1}{j\omega L_L} + j\omega C_R, \quad (9)$$

which is plotted in Fig. 6. The closer to the Γ-point the structure is excited, the more homogeneous (or effective) it is, because $\beta \to 0$ or, in a practical implementation with period a, $a/\lambda_g \to 0$. As rule of thumb, we can consider that the structure is effective from $\beta = 0$ to $\beta = \pi/2a$, where distributed components can be considered lumped, whereas the structure becomes ineffective and strongly anisotropic from $\beta = \pi/2a$ to $\beta = \pi/a$. Metamaterials are concerned with the first case (first half of Γ-X Brillouin zone path).

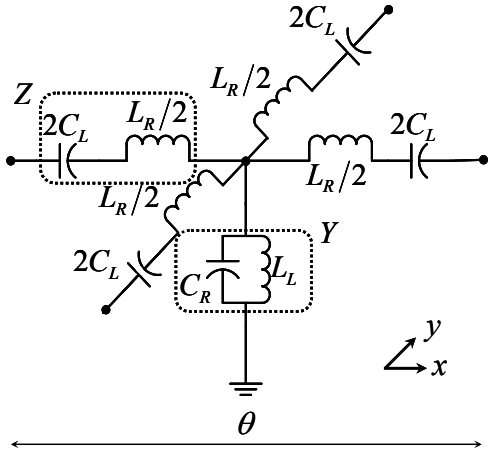

Figure 5: Unit cell of a periodic-network realization of a 2D CRLH-TL. The inductances L_R / L_L and

capacitances C_R / C_L are in H and F, respectively. θ represents the electrical length of the cell (distinct along x and y in anisotropic case).

Since angles are involved in the 2D case, refractive effects can occur. The constitutive parameters, permittivity, permeability and refractive index are given by

$$\varepsilon_r = C'_R - \frac{1}{\omega^2 L'_L} \cong \frac{C_R}{a} - \frac{1}{\omega^2 L_L a}, \qquad (10)$$

$$\mu_r = L'_R - \frac{1}{\omega^2 C'_L} \cong \frac{L_R}{a} - \frac{1}{\omega^2 C_L a}, \qquad (11)$$

$$n = \sqrt{L'_R C'_R} - \frac{c}{\omega^2 \sqrt{L'_L C'_L}} \cong \frac{\sqrt{L_R C_R}}{a} - \frac{c}{\omega^2 \sqrt{L_L C_L}\, a}. \qquad (12)$$

The refractive index can be determined either from (12) after appropriate LC parameters extraction, or more directly from the dispersion diagram with the formula

$$n = \frac{c_0 \beta(\omega)}{\omega}, \quad \beta^2 = k_x^2 + k_y^2 . \qquad (13)$$

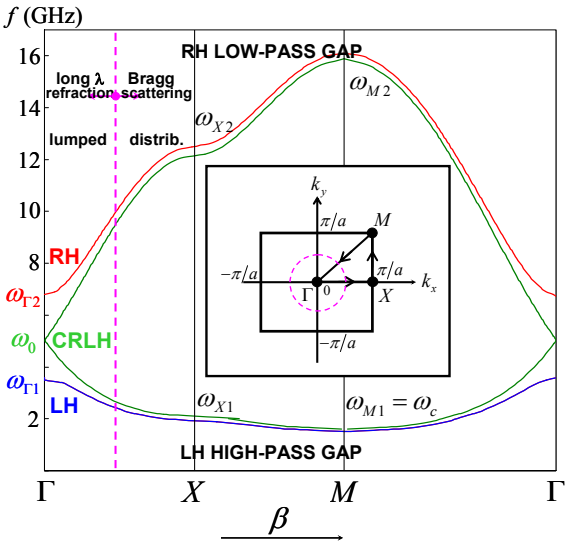

Figure 6: Dispersion relation computed for the balanced and unbalanced 2D CRLH-TL. Balanced: $L_R = L_L = 1$ nH, $C_R = C_L = 1$ pF; unbalanced: $L_R = 1.82$ nH, $L_L = 0.55$ nH, $C_R = 1$ pF, $C_L = 2$ pF. The inset shows the Brillouin zone of the 2D periodic structure.

3. Specific Applications

This section briefly describes four applications, which illustrate the different aspects and usefulness of CRLH structures.

3.1. Dual-Band Branch-Line Coupler

The observation of the CRLH dispersion relation of Fig. 4 (or Fig. 6) reveals that a CRLH-TL provides an additional degree of phase freedom in comparison with the RH-TL, where only the slope of phase can be tuned: it exhibits a DC offset at f_0. Therefore, by simultaneously controlling the phase slope and the DC offset, an arbitrary pair of frequencies with arbitrary electrical length can be obtained in a CRLH-TL. This concept can be introduced in a diversity of components, such as stubs, baluns, phase shifters and couplers to obtain dual-band operation at an arbitrary pair of frequency ranges.

For instance, Fig. 7 presents a branch-line hybrid, in which the RH branches have been replaced by CRLH branches (LH chip sections combined with conventional RH lines in series) [6]. Excellent performances can be obtained in both bands in terms of both magnitude and phase balance without reduction of bandwidth in comparison with the conventional hybrid.

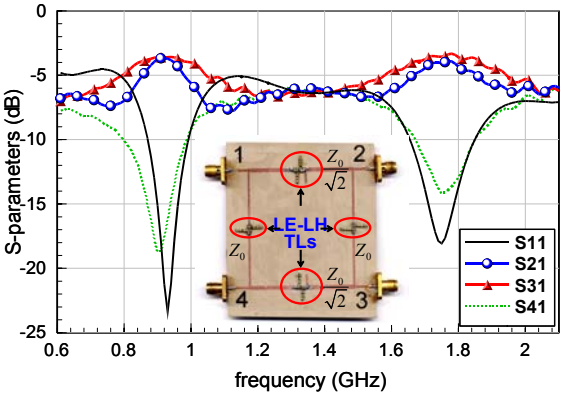

Figure 7: Measured performances of the dual-band inharmonic branch-line coupler. The design frequencies are *920* MHz and *1740* MHz, respectively.

3.2. Coupled-Line Tight Backward Coupler

Combining a CRLH-TL with a conventional RH-TL into a coupled-line configuration results in a backward-wave coupler operating as an

(enhanced) forward coupler (coupling increasing with the electrical length) [4]. This coupler is capable of virtually any loose/tight coupling level. Fig. 8 shows the performances of a prototype achieving quasi *0*-dB (~0.5) over more than *35*% bandwidth. The fundamental principle is that the coherence length, given in conventional couplers by $d_{max} = \pi / |\beta_c - \beta_\pi|$, tends (weak coupling assumption) to become $d_{max} = \pi / [|\beta_{CRLH}| + \beta_{microstrip}]$, because of the fact that the propagation constant of the CRLH-TL is negative in its LH range. Therefore, from the "+" sign, much smaller d_{max} can be achived. A symmetric (quadrature) LH/LH coupler, providing similar performances was also investigated, and observed to be based imaginary even/odd impedances [7]. Both types of coupler can be accurately described by even/odd circuit models.

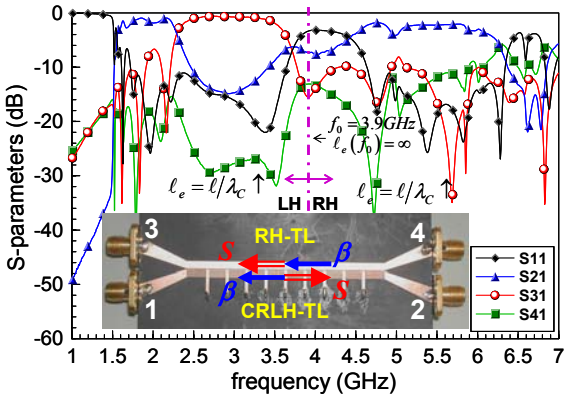

Figure 8: Measured performances of a microstrip RH-CRLH quasi-*0*-dB coupled-line backward coupler with spacing *s=0.3*mm (*s/h=0.19*). The CRLH line is made of series interdigital capacitors and shunt stub inductors. The CRLH transition frequency is f_0*=3.9* GHz. β and *S* represent the propagation constant and the Poynting vector, respectively, in each of the two lines. The same *s/h* provides less then *-10*-dB coupling in the conventional case.

3.3. Backfire-to-Endfire Leaky-Wave Antenna

The backfire-to-endfire leaky-wave antenna is a direct application of the concept of open CRLH-TL described in Sec. 2.2 and Fig. 3 [8]. Radiation patterns for an antenna consisting of the same microstrip CRLH line as that of Fig. 8, terminated by a matched load, are shown in Fig. 9. They demonstrate that the antenna can be scanned both backward (LH) and forward (RH) with broadside radiation at the transition frequency f_0. The unique feature of this antenna is that it fully operates in the dominant mode and that perfect radiation can be obtained at broadside if the design is balanced, since in that case $v_g \neq 0$ (6). Measurements revealed that the antenna can be scanned from backfire to endire in the range from *3.1* to *6.0* GHz.

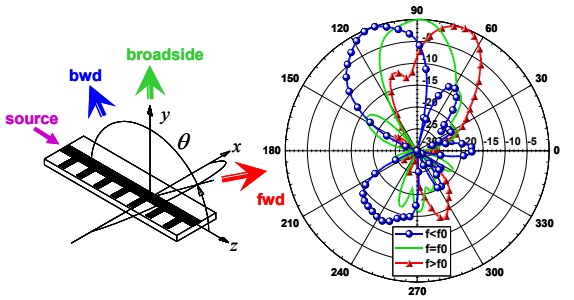

Figure 9: Backfire-to-endfire leaky-wave antenna and radiation patterns at frequencies located in the LH region $f<f_0$ (backward), at the transition frequency $f=f_0=3.9$ GHz (broadside) and in the RH region $f>f_0$ (forward).

3.4. Planar Distributed Negative Refractive Index Lens

A practical distributed implementation of the 2D-CRLH structure of Fig. 5 is the capacitively-enhanced mushroom structure shown in Fig. 10a [9], where caps forming metal-insulator-metal capacitor have been added to the mushroom structure, initially proposed in [10], to increase C_L and therefore force the first dispersion band to become LH (negative slope). A negative refractive index (NRI) planar "lens" was fabricated as the LH capacitively-enhanced mushroom structure sandwiched between two (RH) parallel-plate waveguide structures, as shown in Fig. 10b. The field magnitude and phase measurement results of Fig. 10c clearly demonstrate the expected focusing effect in the center of the NRI structure. The size of the focal point is around $\lambda_0 / 6$.

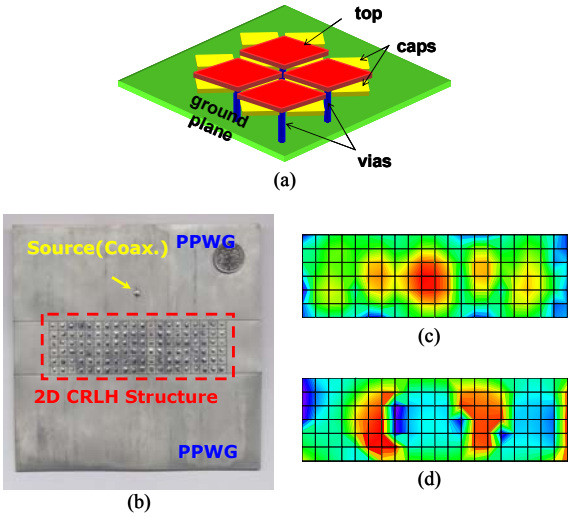

Figure 10: Negative double focusing (negative "lens") using the capacitively-enhanced mushroom LH structure. (a) Perspective view (all shaded areas are metal). (b) Top view of the experimental prototype. (c) Measured vertical electrical field magnitude distribution on top of the lens area. (d) idem for phase.

4. Conclusion

The fundamental theory and practical implementation of CRLH transmission lines and metamaterials has been presented and illustrated by different 1D/2D guided/radiated and refractive applications.

Acknowledgements

This work is part of the MURI program "Scalable and Reconfigurable Electromagnetic Metamaterials and Devices". It was supported by the Department of Defense (N00014-01-1-0803) and monitored by the U.S. Office of Naval Research.

References

[1] V. G. Veselago, "The Electrodynamics of Substances with Simultaneously Negative Values of ε and μ", *Soph. Phys. Usp.,* vol. 10, no. 4, pp. 509-514, January-February 1968.

[2] R. A. Schelby, D. R. Smith, and S. Schultz, "Experimental Verification of Negative Index of Refraction", *Science,* vol. 292, pp. 77-79, April 2001.

[3] C. Caloz, and T. Itoh, "Transmission Line Approach of Left-Handed (LH) Structures and Microstrip Realization of a Low-Loss Broadband LH Transmission Line", submitted to *IEEE Trans. Ant. Propagat.*

[4] C. Caloz and T. Itoh, "Novel microwave devices and structures based on the transmission line approach of meta-materials," *IEEE-MTT Int'l Symp. Digest*, pp.195-198, Philadelphia, PA, June 2003.

[5] C. Caloz, and T. Itoh, "Application of the Transmission Line Theory of Left-Handed (LH) Materials to the Realization of a Microstrip LH Transmission Line", *IEEE-APS Int'l Symp.,* vol. 2, pp. 412-415, San Antonio, TX, June 2002.

[6] I. Lin, C. Caloz and T. Itoh, "A Branch-Line Coupler with Two Arbitrary Operating Frequencies Using Left-Handed Transmission Lines", *IEEE-MTT Int'l Symp.,* vol. 1, pp. 325-327, Philadelphia, PA, June 2003.

[7] C. Caloz, A. Sanada, L. Liu and T. Itoh, "A Broadband Left-Handed (LH) Coupled-Line Backward Coupler with Arbitrary Coupling Levels", *IEEE-MTT Int'l Symp.,* vol. 1, pp. 317-320, Philadelphia, PA, June 2003.

[8] L. Liu, C. Caloz, and T. Itoh, "Dominant Mode (DM) Leaky-Wave Antenna with Backfire-to-Endfire Scanning Capability", *Electron. Lett.,* vol. 38, no. 23, pp. 1414-1416, Nov. 2000.

[9] A. Sanada, C. Caloz, and T. Itoh, "2D distributed meta-structures with negative refractive properties," *IEEE AP-S USNC/URSI Digest*, vol. 1, Columbus, OH, June 2003.

[10] D. Sievenpiper, L. Zhang, R. F. J. Broas, N. G. Alexopolous, and E. Yablonovitch, "High-Impedance Electromagnetic Surfaces with a Forbidden Frequency Band", *IEEE Trans. Microwave Theory Tech.,* vol. 47, no. 11, pp. 2059-2074, Nov. 1999.